

Laboratory investigation of a three dimensional wall attached density current down an inclined slope in a rotating tank

N.E. Kotsovinos & P. Kralis

School of Engineering, Democritus University of Thrace, Xanthi, Greece

ABSTRACT : The time dependent three dimensional wall attached density current down an inclined plane surface in a large tank, rotating anticlockwise, is studied experimentally. As expected, the density current is deflected to the right. There is a initial regime (regime A) where the angle of the deflection is almost constant and obtains large values (up to 70 degrees). The regime A is followed by another regime (regime B), where the angle of deflection is smaller. The transition time from regime A to regime B is equal to about one rotation period. The angle of the deflection depends from the Rossby radius of deformation. For the configuration of our experiments the predominant driving force is the gravity.

1. INTRODUCTION

The objective of this paper is the laboratory study of the spreading of three dimensional dense gravity current down an inclined plane surface in a large tank rotating anticlockwise with angular velocity Ω . This flow simulates the bottom outflow of dense deep ocean water from an elevated strait. The dense outflow sinks and spreads over the sloping ocean bottom. The dynamics of this flow is influenced by the earth rotation due to the scale of the problem. The rotation of the earth alters the path and structure of the gravity current. This flow is important from the environmental point of view because the density current may transport sediment or pollutant deposited at the sea floor. The geometry of the problem is shown in Figures 1a, 1b and 1c. The outflow volume flux that feeds the gravity current is Q . The entrainment in the gravity current is assumed small so that we may assume that to the first approximation the conservation of mass gives:

$$HSB \sim Qt \quad (1)$$

where H is the thickness, B the width and $S(t)$ the distance of the foremost point of the front, measured along the deflected centerline longitudinal trajectory. The trajectory of the spreading gravity current down an inclined plane surface of slope with the horizontal plane equal to θ (see Figure 1a) results from the balance of five forces: the gravity force F_g , the pressure force F_p , the inertia force F_i , the Coriolis force F_c and the friction (mainly bottom friction) force F_d . The forces which drive the flow are two: the gravity force F_g , and the pressure (or buoyancy) force F_p . The forces which retard (or resist) the flow are three: the inertia of the gravity current F_i , the Coriolis force F_c and the friction force F_d . The methodology that we follow to find the asymptotic growth rate of the length $S(t)$ with time is based on the balance of the forces which drive and retard the flow. Similar methodology has been used previously by Chen and List (1976), and Lemkert and Imberger (1993). Subsequently we find the scaling of the above mentioned forces, where the continuity equation (1) has been considered and where the typical horizontal velocity U of the front is given by S/t , where t is the time.

The pressure inside the gravity current is clearly greater than the pressure outside. To the first approximation the excess pressure force F_p is given by

$$F_p = \text{pressure (or buoyancy) force} = O(\rho'gH^2 B \cos\theta) = O(\rho'gB^{-1}Q^2 S^{-2} t^2 \cos\theta) \quad (2)$$

where ρ' is the excess density . The scaling of the other forces is given subsequently.

$$F_g = \text{gravity force} = O(\rho' g H B S \sin \theta) = O(\rho' g Q t \sin \theta) \quad (3)$$

$$F_i = \text{inertia force} = O(\rho H B U^2) = O(\rho Q S t^{-1}) \quad (4)$$

$$F_c = \text{Coriolis force} = O(\rho H B S f U) = O(\rho Q f S) \quad \text{where } f = \text{the Coriolis parameter} = 2\Omega \quad (5)$$

We assume that the drag force is mainly due to bottom shear

$$F_d = O(\mu U H^{-1} B S) = O(\mu B^2 S^3 Q^{-1} t^{-2}) \quad \text{where } \mu \text{ is the dynamic viscosity} \quad (6)$$

It is apparent that the magnitude of the above forces vary with time and with the length S . The ratio of the Coriolis force becomes larger than the inertia force when

$$\frac{F_c}{F_i} = f t > 1 \quad \text{or when } t > 0.08 \text{ rotation periods} \quad (7)$$

The driving gravity force becomes larger than the pressure force when

$$\frac{F_g}{F_p} = \frac{Q t \sin \theta}{Q^2 B^{-1} S^{-2} t^2 \cos \theta} = Q^{-1} B S^2 t^{-1} \tan \theta = S H^{-1} \tan \theta > 1 \quad \text{or} \quad \tan \theta > H/S. \quad (8)$$

The experiments of this study satisfy the above relationship (e.g. $\tan \theta = 0.06$ and 0.12 ; visual observations indicate that in these experiments the thickness H is less than $0.06 S$).

We examine subsequently the following balance of the driving and resisting forces:

i) **Regime A:**

In this regime the driving gravity force is larger than the pressure driving force ,and the resisting Coriolis force is larger than the inertia force and larger than the drag force . We have therefore a balance of the driving gravity force F_g and the resisting Coriolis force F_c : i.e. $F_g = F_c$, so that we obtain:

$$S_A = C_A (\rho' g / \rho_s) f^{-1} \sin \theta \quad \text{where } C_A \text{ is an experimental constant} \quad (9)$$

ii) **Regime B:**

In this regime we have a balance of the gravity driving force F_g and the resisting friction force F_d , and we obtain:

$$B^2 S^3 \approx (\rho' g / \rho) \nu^{-1} Q^2 t^3 \quad (10)$$

In these experiments is not a good approximation to assume self similarity, and it is not easy to assume a relationship between B and H . We prefer to estimate from the contours the growth rate of the area of spreading , which is assumed equal to BS . We found in these experiments that

$$B S \approx t^m \quad \text{where } m \sim 1 \text{ to } 1.15 \quad \text{Therefore equation 10 gives} \quad (11)$$

$$S \approx (\rho' g / \rho) \nu^{-1} Q^2 t^n \quad \text{where } n = 0.85 \pm 0.15 \quad (12)$$

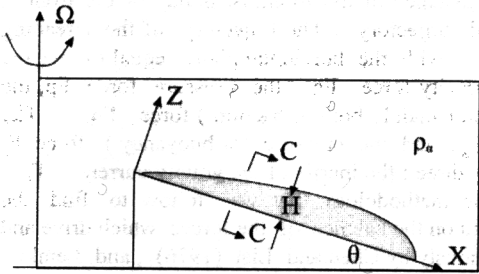


Figure 1a : Side view

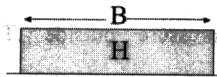


Figure 1b : section cc

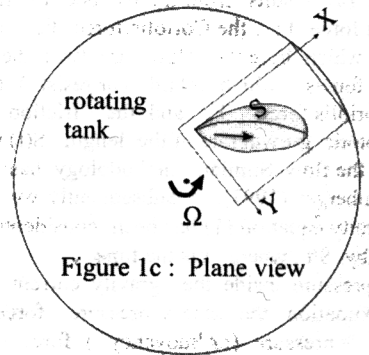


Figure 1c : Plane view

3. EXPERIMENTAL PROCEDURE - EXPERIMENTAL RESULTS

The experiments were made in a large rotating tank (diameter 5.2 m) containing a inclined glass wall mounted on the tank floor. The tank was filled with tap water and was rotating for about three hours to achieve ambient fluid motionless and rotating as a solid body. The bottom gravity current was produced by continuously injecting, at the top of the inclined plane, colored salt water of density ρ_0 at constant volume flux through a pipe of diameter $D=3.5$ mm. A substantial number of experiments were performed (80 experiments), where we vary the slope of the inclined plane (inclination angle with the horizontal $\theta=3.52^\circ$ and $=6.9^\circ$), the initial volume flux of the injected salt water Q from $2.73 \text{ cm}^3/\text{s}$ to $5.16 \text{ cm}^3/\text{s}$ and the Coriolis parameter f from 0.105 sec^{-1} to 0.465 sec^{-1} . For comparison we run a few experiments without rotation of the tank. The initial Richardson number of the gravity current Ro is defined as $Ro = \frac{\mu\beta}{m^{3/4}}$ where μ , β and m the kinematic fluxes of mass,

buoyancy and momentum at the origin of the gravity current and varied from 0.048 to 0.13. The Rossby number $=U/fS$, calculated using the mean velocity of the front, varied from 0.082 to 0.51. The characteristic baroclinic Rossby deformation radius $ro = \left(\frac{\rho g H}{\rho} \right)^{1/2} / f$ calculated for a typical thickness H of the gravity current equal to 1 cm, varied

from 9 to 62 cm. The characteristic inertial radius $ri=U/f$ varied from 1.96 to 12.27. The ratio ri/ro (\sim densimetric Froude number) varied from 0.09 to 0.39.

The main emphasis of these experiments is to determine the trajectory of the gravity current as a function of time. The gravity current was recorded continuously using a color video camera. Typical contours of the spreading of the gravity current every 10 sec is shown in Figure 2.

The Cartesian Coordinates $X(t)$ and $Y(t)$ of the position of the front of the spreading are plotted in Figure 3 (for non rotating tank the coordinate $Y(t)$ of the foremost point of spreading front is zero). It is observed that there are at least two basic regimes. The initial regime A is characterized by a substantial deflection of the trajectory to the right. The angle of the deflection ω_A in this regime from various experiments is plotted in Figure 4 as a function of the Rossby deformation radius ro . We observe that the deflection angle ω_A decreases with increasing ro .

The regime A is followed by the regime B where the deflection angle is ω_B . We observe that $\omega_A > \omega_B$ (see Figures 2, 3 and 4). The best fit line between the deflection angles ω_A and ω_B and the deformation radius gives

$$\omega_A = 360/ro^{0.6}$$

and

$$\omega_B = 160/ro^{0.64}$$

The transition time T_c which characterizes the transition from regime A to regime B, divided by the

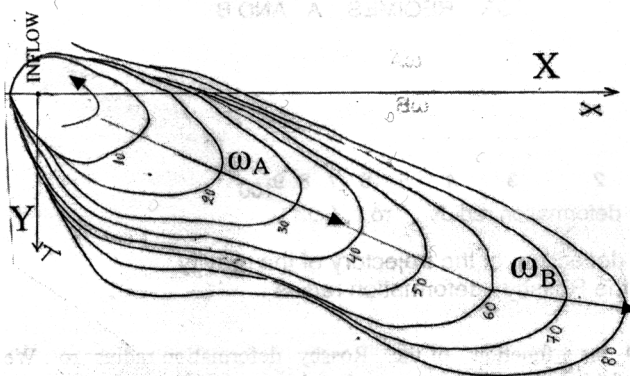


Figure 2 Contours of the gravity current as a function of time; $Q=4.33 \text{ cm}^3/\text{s}$, $\theta=6.9^\circ$, rotation period 45.5 sec, $\rho'=0.029 \text{ gr/cm}^3$

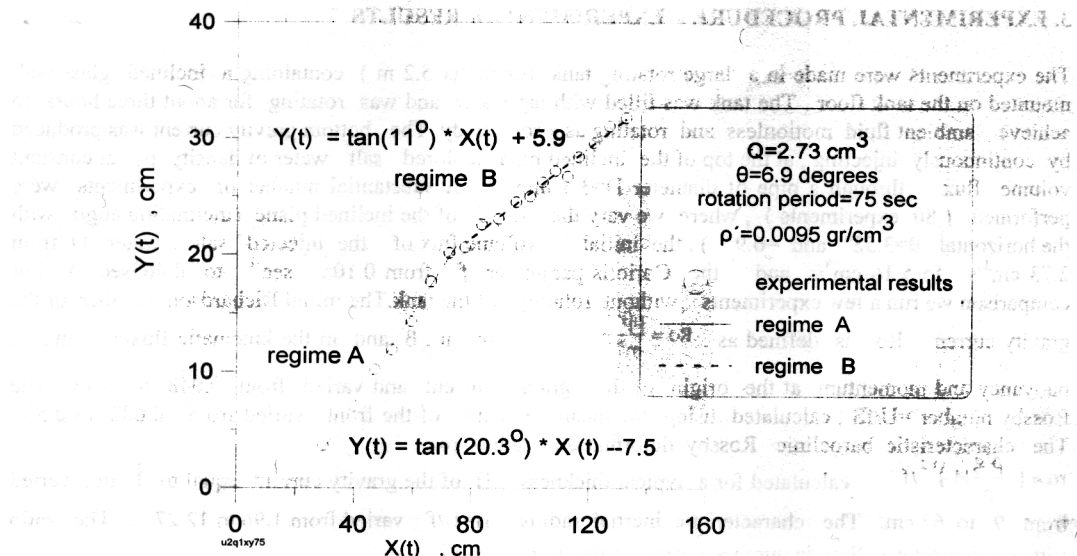


Figure 3 The Cartesian Coordinates $Y(t)$ and $X(t)$ of the front of the gravity current as a function of time t . The transition time T_c from regime A to regime B is about one rotation period ,i.e. about 75 sec.

In regime A the deflection angle is $\omega_A = 20.3^\circ$, and in regime B is $\omega_B = 11^\circ$

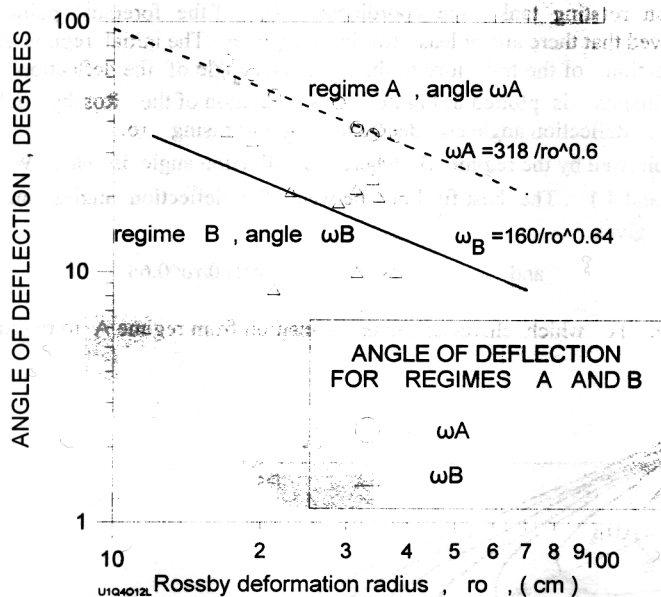


Figure 4 The angle of deflection of the trajectory of the gravity current as a function of the Rossby deformation radius .

rotation period T , is plotted in Figure 4 as a function of the Rossby deformation radius ro . We observe that there is a weak dependence of this transition from ro , but that to the first approximation the transition from regime A to regime B occurs at a time equal to about one rotation period. The position of the foremost point of the front of the gravity current as a function of time is found

for each experiment from the corresponding contour . These foremost points determine a trajectory which is used to measure the length $S(t)$ of the foremost point of the front . The length of the trajectory of the front spreading $S(t)$ is plotted as a function of time t in Figure 5 using the experimental data which were used to plot Figure 3 . We observe the appearance of two regimes in the growth rate of $S(t)$. The transition occurs at the same location where we observed from Figure 3 the transition from regime A to regime B , i.e . at the location where we have a change in the magnitude of the deflection angle . Two straight lines are fitted to the experimental data in Figure 4 , one for the regime A and the other for the regime B . The corresponding equations of the fits are printed in the Figure 4 and are given subsequently:

$$\text{regime A (gravity-Coriolis) } S(t) = 0.74t + 17.2 \quad (13)$$

$$\text{regime B (gravity-viscous) } S(t) = 0.5t + 37.1 \quad (14)$$

We observe that the fitting equation for the regime A is of the form $S(t) \sim t$, and is compatible with the theoretical equation (9) which for a balance of the driving gravity force and resisting Coriolis force give that $S(t)$ increases linearly with time . The growth rate of $S(t)$ in regime B (gravity-viscous) is in this example linear function of time ; however in this regime the longitudinal growth $S(t)$ depends directly from the growth of the width B (see equation 11) .

Finally, in some experiments we observed the lateral growth (to the right of the flow) of large instabilities which used to grow with time to produce minor secondary trajectories , with small volume flux , but large deflections angles to the right , almost perpendicular to the main stream of flow.

6. CONCLUSIONS

The macroscopic experimental observations of the trajectory and the contours of the gravity current down the inclined plane surface in a rotating tank reveal the appearance of various regimes and lateral instabilities (or secondary flows) . This preliminary study indicate a correlation of the deflection angle with the Rossby deformation radius ro . The inclination of the plane bottom in these experiments was

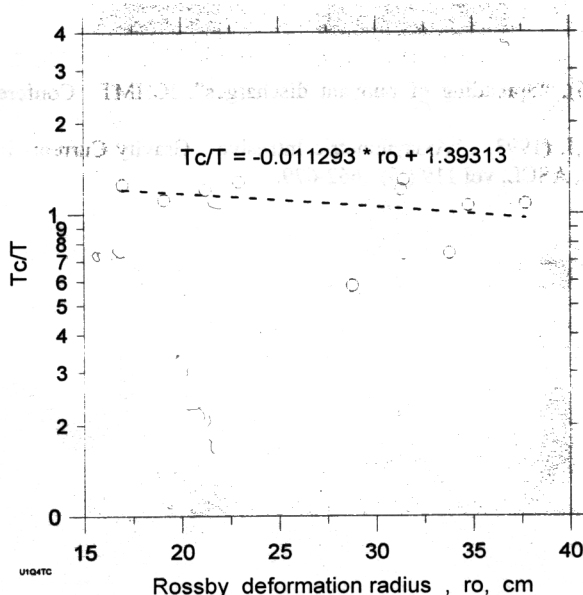


Figure 5. The transition time T_c from regime A to regime B (transition of deflection angle from ω_A to ω_B), divided by the rotation period of the tank T , is plotted as a function of Rossby deformation radius.

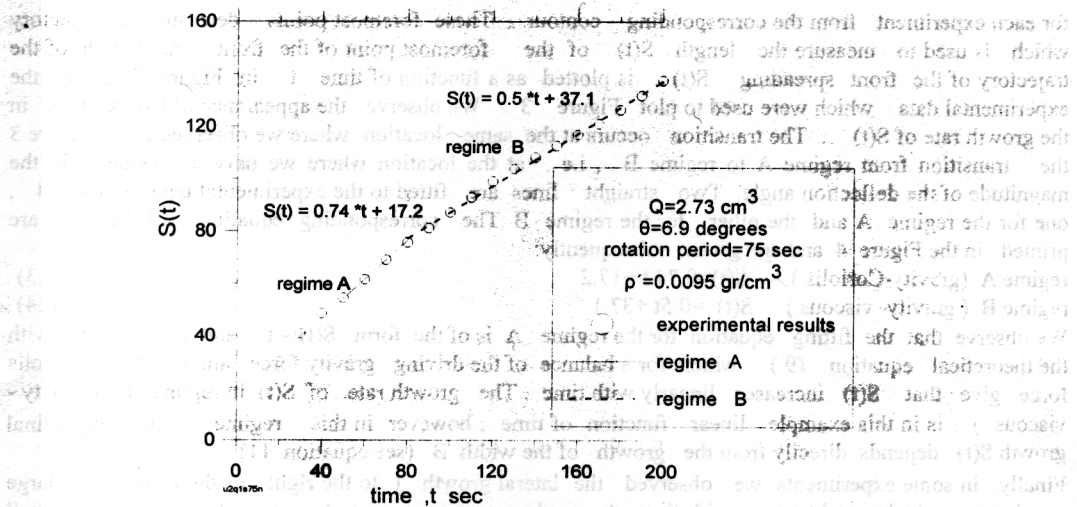


Figure 6 The growth rate $S(t)$ of the axial distance of the front of the gravity current as a function of time t . The rotation period is 75 sec and therefore for this plot $0.26 < t/T < 2.6$. The transition from regime A to regime B occurs at time equal to one rotation period.

relatively high, so that the driving gravity force was balanced with the resisting Coriolis force, giving a regime where the distance along its trajectory of the foremost point of the front grows linearly with time. It appears also that at time t equal about to one rotation period there is a substantial change in the deflection angle of the trajectory. It seems that at that time the gravity-Coriolis regime changes to gravity-viscous regime.

REFERENCES

- Chen, J.C., and List, E.J. (1976), "Spreading of buoyant discharges", ICHMT Conference, Dubrovnik, Yugoslavia, 171-182.
- Lemkertt, C.J. and Imberger, J. (1993), "Axisymmetric Intrusive Gravity Currents in linearly Stratified Fluids", J. Hydraulic Engrg., ASCE, vol 119 (6), 662-679.